Proton transfer mechanism of 1,3,5-tri(2-benzimidazolyl) benzene with a unique triple-stranded hydrogen bond network as studied by DFT-MD simulations

ARTICLE *in* CHEMICAL ENGINEERING SCIENCE · DECEMBER 2015

Impact Factor: 2.34 · DOI: 10.1016/j.ces.2015.07.001

Chemical Engineering Science 137 (2015) 404–411

Contents lists available at ScienceDirect

Chemical Engineering Science

journal homepage: www.elsevier.com/locate/ces

Proton transfer mechanism of 1,3,5-tri(2-benzimidazolyl) benzene with a unique triple-stranded hydrogen bond network as studied by DFT-MD simulations

Piyarat Nimmanpipug [a,*], Teerawit Laosombat [a], Vannajan Sanghiran Lee [a,b], Sornthep Vannarat [c], Suwabun Chirachanchai [d], Janchai Yana [e], Kohji Tashiro [f,*]

[a] Computational Simulation and Modeling Laboratory (CSML), Department of Chemistry, Faculty of Science, Chiang Mai University, Chiang Mai 50200, Thailand
[b] Department of Chemistry, Faculty of Science, University of Malaya, Kuala Lumpur 50603, Malaysia
[c] Large Scale Simulation Research Laboratory, National Electronics and Computer, Technology Center, Pathumthani 12120, Thailand
[d] The Petroleum and Petrochemical College, Chulalongkorn University, Bangkok 10330, Thailand
[e] Department of Chemistry, Faculty of Science and Technology, Chiang Mai Rajabhat University, Chiang Mai 50300, Thailand
[f] Department of Future Industry-Oriented Basic Science and Materials, Graduate School of Engineering, Toyota Technological Institute, Nagoya 468-8511, Japan

HIGHLIGHTS

- Proton transfer in a benzimidazole derivative with a unique packing was simulated.
- Partial charge alteration due to electric field perturbation was elucidated.
- Proton hopping mechanism related with hydrogen bond network was suggested

ARTICLE INFO

Article history:
Received 19 March 2015
Received in revised form
31 May 2015
Accepted 1 July 2015
Available online 9 July 2015

Keywords:
Benzimidazole
Hydrogen bond network
Proton transfer
Density functional molecular dynamics simulations
Fuel cell

ABSTRACT

Clarification of proton transfer mechanisms is crucial to the development of proton exchange membrane fuel cells (PEMFCs). Nitrogen-containing heterocyclic compounds (*e.g.*, imidazole derivatives) are well known for their potential to assist proton hopping through hydrogen bond networks at high temperatures. Among the many imidazole derivatives reported thus far, 1,3,5-tri(2-benzimidazolyl)benzene (TBIB) is assumed to be one of the most promising imidazole derivatives because of its triple-stranded three-dimensional hydrogen bond network. In fact, TBIB immersed into a polyphosphoric acid matrix was reported to enhance the proton conductivity to 10^{-2}–10^{-1} S/cm in the high-temperature range up to 170 °C. In the present work, the proton transfer mechanism has been investigated using density functional theory (DFT) with a DNP basis set and the GGA exchange-correlation functional BLYP and molecular dynamics simulations (MD) to provide insight into the cause of the remarkable proton conductivity of TBIB. Transition states in the proton hopping process were obtained using two types of models constructed from the X-ray crystal structure: an isolated two-molecule system (type I) and a periodic three-molecule system (type II). Alterations of charge distribution, molecular conformation and molecular orientation were investigated from these models. Further, the diffusion coefficient of proton transfer has been estimated and the mechanisms along three specific channels that favor efficient proton transfer between the layers have been examined in detail. Additionally, the effect of an electric field perturbation was investigated for these two models. The application of an external electric field was found to affect the proton hopping process remarkably, as evidenced by large changes in the activation energies and proton hopping times. In conclusion, the highly organized hydrogen-bonding network observed for TBIB was found to be a key factor in enhancing the efficiency of proton transfer.

1. Introduction

For several decades, research and development of fuel cells as alternative technologies for green energy have attracted considerable attention. Proton exchange membrane fuel cells (PEMFCs) are a

Abbreviations: DFT-MD, density functional theory-molecular dynamics; BENZIM, benzimidazole; PEMFC, proton exchange membrane fuel cell

* Corresponding authors.
E-mail addresses: piyaratn@gmail.com (P. Nimmanpipug), ktashiro@toyota-ti.ac.jp (K. Tashiro).

http://dx.doi.org/10.1016/j.ces.2015.07.001
0009-2509/

promising technology for use in transportation and portable power sources (Smitha et al., 2005). A critical component of this technology is the proton exchange membrane (PEM), (Devanathan, 2008) which is used to separate the reaction products and enable proton transfer between the electrodes in the PEMFC. Among the various types of materials used as a PEM, Nafion® has been widely employed because of its high proton conductivity and chemical resistance (Devanathan, 2008; Jeong et al., 2006; Choi et al., 2005; Yan et al., 2007). Several studies have demonstrated the correlation between water concentration and proton conductivity of Nafion®. Moreover, hydration is mandatory for proton transfer in Nafion, and so its conductivity decreases drastically when the operation temperature is too high (Gosalawit et al., 2006). Consequently, a molecular design of an alternative electrolyte membrane, which can be used at high operation temperatures, would be of great benefit.

In this regard, nitrogen-containing heterocyclic compounds, *e.g.*, imidazole, benzimidazole and pyrazole, have previously been investigated to elucidate their interesting chemical and physical properties (Schuster et al., 2001; Pangon et al., 2011; Kawada et al., 1970; Kreuer et al., 1998; Agmon, 1995). One notable property of these compounds is their ability to transfer protons without hydration via their hydrogen bond network (Schuster et al., 2001; Yamada and Honma, 2005). In this case, hydrogen bonds formed between neighboring rings have been considered to be vital for the proton transfer pathway. By analyzing the character of the hydrogen bond network, the role of each hydrogen bond can be discerned to understand and control the proton transfer process (Isaev, 2012; Ishikita and Saito, 2014). For imidazole (Münch et al., 2001), a proton transfer mechanism involving protonation of the nitrogen atom associated with the re-orientation of imidazole molecules along a hydrogen bond axis was proposed, by which the proton transfer can be accelerated at higher temperatures. Schuster et al. (2001) investigated imidazole with an acidic proton in a membrane and with the imidazole immobilized on ethyleneoxide oligomers. A comparison of proton conductivity and NMR diffusion coefficients between pure and acid-doped compounds indicated that the diffusion of molecules dominates the conduction process, which gives a proton conductivity above the melting point ($>120\ ^{\circ}C$) in completely water-free materials. This result suggests that the proton transfer of an imidazole system is based on proton hopping, as in the Grotthuss mechanism (Fig. 1a; Agmon, 1995). In the case of proton transfer between the imidazole molecules, charge defects were also proposed to be involving (Fig. 1b; Kawada et al., 1970). As a result, proton exchange occurs very rapidly between the ionic and neutral imidazole molecules along the hydrogen-bonded axis. The movement of the proton to the electrode occurs through properly oriented hydrogen bonds *via* a thermally generated positive ion state.

These experimentally deduced proton transfer models must be supported from a theoretical point of view. In general, molecular dynamics simulations give trajectories that specify how the position and velocities of each atom in the system vary with time at various temperatures. Agmon (1995) suggested a mechanism of proton motion based on quantum mechanical calculations and Monte Carlo and molecular dynamics simulations. They found that proton migration occurs as a hydrogen-bond cleavage process in front of the moving proton and as a hydrogen bond formation process at the back of the proton. Münch et al. (2001) studied the diffusion mechanism of an excess proton in imidazole chains by a Car-Parrinello-type *ab initio* molecular dynamic simulation. In this case, the proton diffusion process was rationalized by the Grotthuss-type diffusion mechanism. The transport of the excess proton in the imidazole chain was speculated to include the proton transfer steps and a reorientation of the imidazole molecules. To elucidate the proton transport and diffusion dynamics, DFT-MD has been utilized and the results have been compared with experimental data of proton conductivity (Chen et al., 2009; Li et al., 2012; Tölle et al., 2008; Ludueña et al., 2011; Peterson et al., 2013).

In addition, there are number of simulation studies that have indicated that an external electric field shifts the equilibrium of proton transfer toward the direction of electrostatic attraction. Hermansson and Ojamäe (1995) studied the influence of uniform and non-uniform electric fields on the proton transfer process between two water molecules using *ab initio* calculations. The results indicated that the proton transfer barrier is greatly reduced by the application of an electric field of 0.0050 a.u. (2.5×10^7 V/cm). Based on DFT-simulations, Ohwaki and Yamashita (2001) studied the electric field effects on the proton transfer reaction that occurs on electrode surfaces. In our previous study, proton transfer mechanisms of water and imidazole molecules were investigated by DFT-based MD simulations (Nimmanpipug et al., 2013). In this case, excess protons were doped to the proton donor that generates an electric dipole in the system. An electric field applied to the opposite direction to the system dipole was found to reduce the activation energy for the proton transfer process. In addition, the DFT-MD simulations of the bulk system show that the perturbation of an applied electric field in the range 0.0025–0.0075 a.u. (1.29×10^7–3.86×10^7 V/cm) increased the proton diffusion coefficient in both water and imidazole systems. Moreover, the reorientation of the imidazole molecules during proton hopping led to a tilt of the proton hopping direction in the imidazole crystal structure.

On the basis of these results, we have been inspired to investigate the $(C_6H_3)(C_7H_5N_2)_3$ and 1,3,5-tri(2-benzimidazolyl) benzene (TBIB) systems, as will be reported in the present paper. This imidazole derivative has been reported to adopt a unique helical packing crystal structure with triple-stranded hydrogen bond networks, as shown in Fig. 2.

The tetragonal-type unit cell parameters of TBIB are: $a=b=24.95$ Å and $c=46.61$ Å. The space group is *P-4n2*, in which the 4 columns are included, and there are 13 molecular layers included in one column Tashiro et al., 2009.

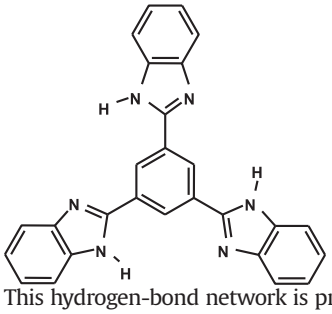

This hydrogen-bond network is proposed to enhance the cooperative proton conductivity along the helical axis. In fact, this crystal structure has one of the most highly developed proton hopping abilities on record (Pangon et al., 2011). In the present paper, the proton transfer mechanism for this unique structure will be investigated using density functional theory. We note that this structure was also reported to have a melting point above 200 °C, and high proton conductivity was detected up to the appreciably high temperature region of 25–200 °C. The present calculations provide a detailed mechanism of such high proton conductivity for TBIB. It is expected that these results will guide the development of highly organized hydrogen bonding networks involving imidazole.

2. Methodology

Two types of models were constructed to understand the proton transfer mechanism of TBIB system.

2.1. Development of the type-I model

Initially, a pair of two TBIB molecules from the crystal structure (Fig. 3) was chosen as an isolated system and one proton was added

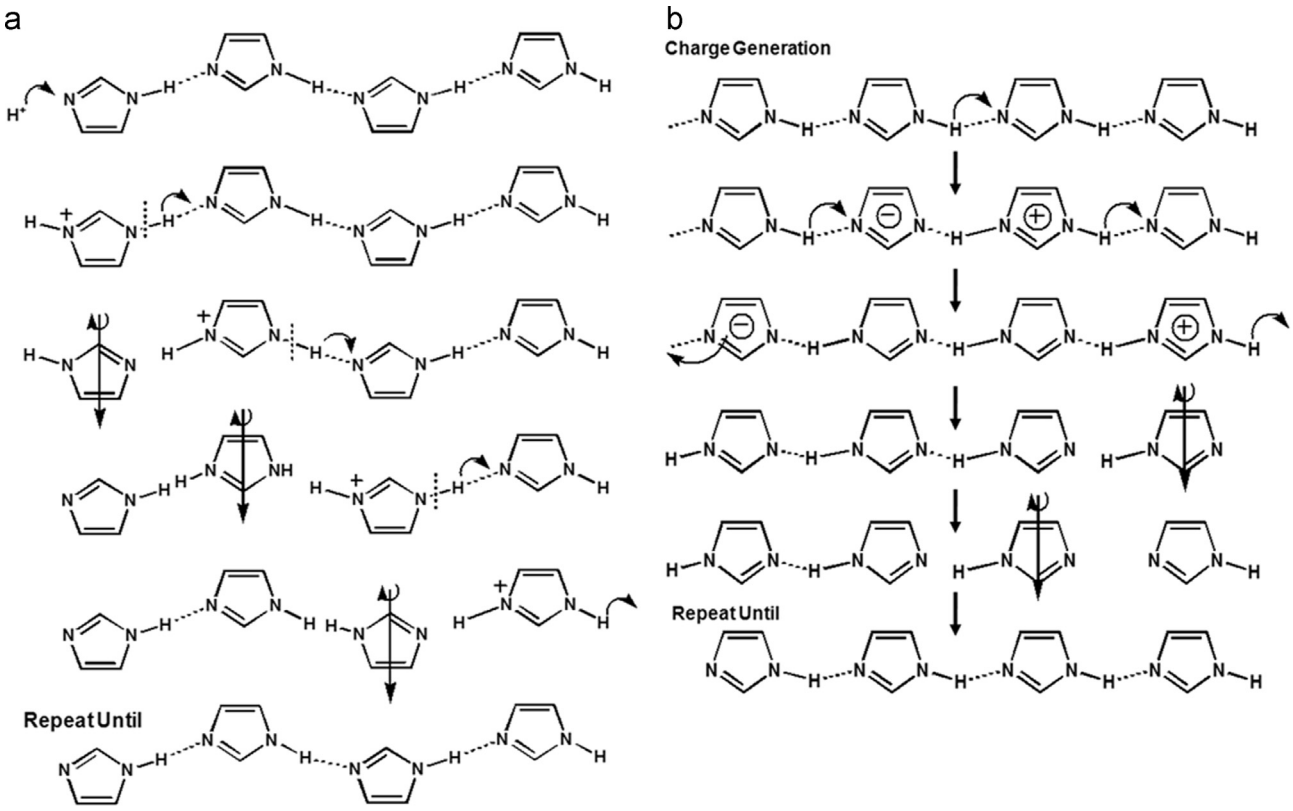

Fig. 1. Proton transfer models in neighboring imidazole rings. (a) Grotthuss model (Agmon, 1995) and (b) charge defect model (Kawada et al., 1970).

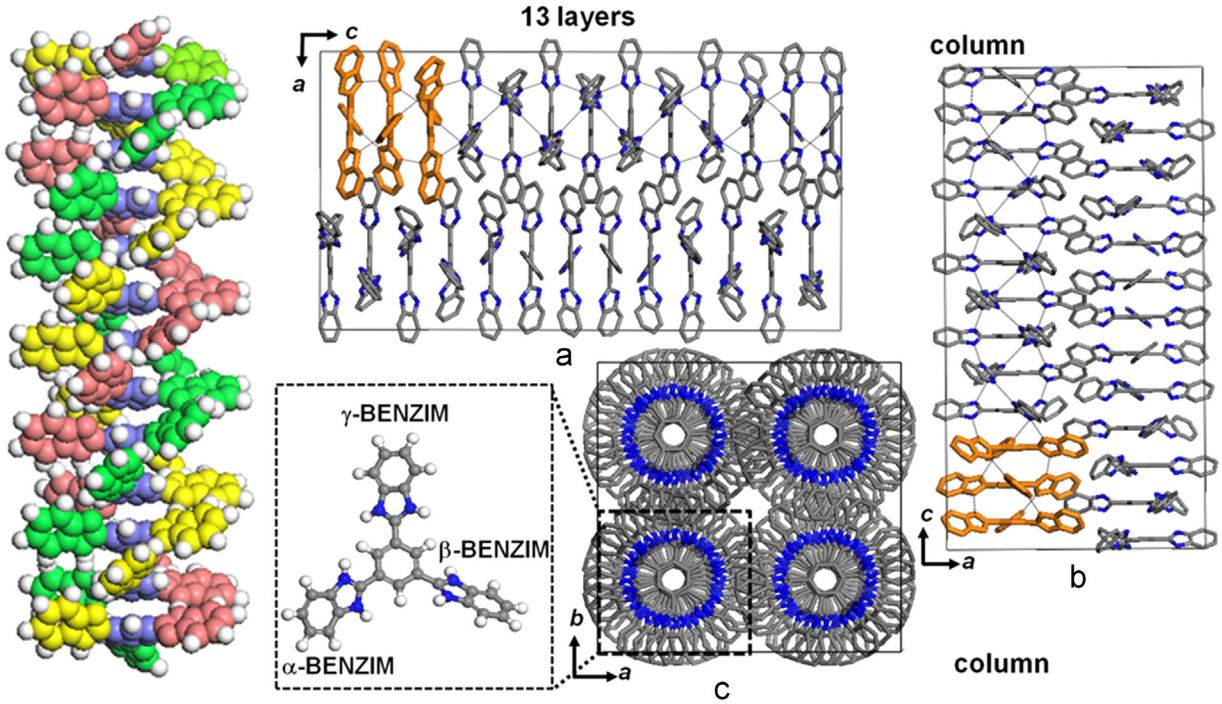

Fig. 2. Crystal structure of TBIB projected in the (a) ac-plane, (b) bc-plane and (c) ab-plane.

to the 1st molecule. All of the electrons within the H, N and C atoms were explicitly accounted for in these calculations, and the basis set included polarization functions. Proton transfer was investigated using transition state searches using the GGA density functional BLYP with double numerical basis set with p polarization functions on all of the hydrogen atoms (DNP). DMol^3 of the Materials Studio version 5.5 program (Accelrys, USA) was used to perform the calculations (Studio, 2011). Complete LST/QST (Linear Synchronous Transit/Quadratic Synchronous) profiles were used to calculate the reaction paths between the reactants and products. The reactants

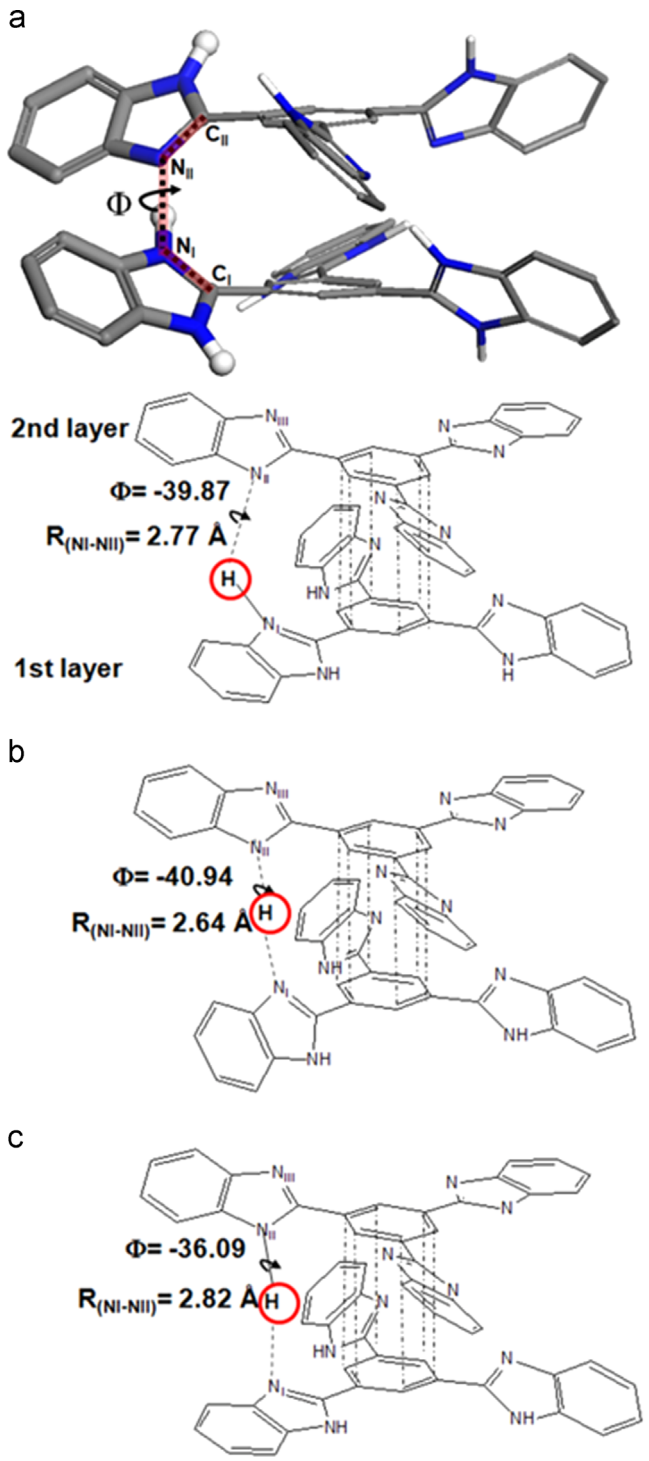

Fig. 3. Proton transfer mechanism in an isolated TBIB model (type I) (a) reactant, (b) transition state and (c) product.

and products were optimized with the BLYP exchange-correlation functional with an SCF tolerance of 1.0×10^{-6}. Additionally, the effect of an external electric field on the proton transfer in the system was examined along the proton transfer path in the *c* direction of the electric field strength.

2.2. Development of the type-II model

The proton transfer mechanism has been investigated by density functional theory (DFT) with the DNP basis set and the BLYP exchange-correlation functional with molecular dynamics simulations (MD) to elucidate the cause of the remarkable proton conductivity of TBIB. The mechanisms in three specific channels for the smallest unit have been revealed within 2 ps. The results suggest efficient proton transfer between the layers in a columnar arrangement, indicating a high proton conductivity of the materials. Repeating these calculations with additional layers and longer time scales remain under investigation; however, large simulation cells may present other associated problems. In general, larger length-scale motions of atoms will be associated with longer time scales, which can make relaxation or equilibration difficult to obtain. There are other approaches (*e.g.*, multiscale modeling) where detailed modeling with a high level of theory is performed for a small region that is embedded into a region that is modeled with less accurate level of theory. However, the current approach of using the smallest unit provides straightforward insight into the proton transfer mechanism for the systems with and without an external electric field.

In the type-II model, as shown in Fig. 4, three molecules were extracted from the crystal structure along the *c* direction. Three excess protons were added to the first layer to protonate the system. The basic box containing 3 molecules had the dimension of $12.5\times12.5\times10.8$ Å^3. Prior to the MD simulations, the cell parameters and model structure were optimized with BLYP and the DNP basis set in Dmol^3. The molecular structures following geometry optimization differ slightly from the initial structures: the optimized box dimensions are $a=15.05$ Å, $b=12.69$ Å, $c=13.78$ Å and the root-mean-square deviation of the atomic displacements is 1.18 Å.

The canonical MD simulations were performed with P1 space-group symmetry so that all structures are fully relaxed. The fully relaxed structure was found to be well correlated with the crystal structure. An NPT ensemble was not applied in the present calculations because variable-cell DFT simulations typically require a larger cut-off energy to converge properly. A Nose–Hoover thermostat set to 298 K was applied. A time step of 1 fs was used for 2.0 ps of total simulation time. Additionally, the effect of an increasing electric field was examined in the DFT-MD simulations, as described in Section 2.1 for the isolated system. The proton diffusion coefficient in the hopping process was calculated by estimating the slope of the mean square displacement (MSD) with the function of time (t) following the Einstein relation (Kreuer et al., 1998; Kubo 1957):

$$D=\frac{1}{6}\left[\frac{\left\langle [R(t)-R(0)]^2\right\rangle}{t}\right]_{t\to\infty}$$

3. Results and discussion

3.1. Proton transfer in the isolated system (type-I model)

3.1.1. Energy profile and transition state structure for proton transfer

The geometrical change during the proton transfer process was investigated by calculating the inter-molecular torsion angle (Φ) and intermolecular distance (R_{N-N}, R_{N-H} and R_{H-N}) for the reactant, the transition state and the product, as shown in Table 1. Here, the torsional angle Φ is defined as the angle between the two C–N bonds (N_I–C_I and N_{II}–C_{II}) formed between the two hydrogen bonded rings shown in Fig. 3. The change of Φ of each structure suggests that the benzimidazole rings were slightly twisted from -39.81° to -40.94° to adjust the inter-molecular distance (R_{NI-NII}) from 2.77 Å (reactant) to the critical distance of 2.64 Å (in the transition state) so that the proton transfer occurs. After the proton was transferred to the 2nd layer, the R value returned to the original layer value (2.82 Å, product). The change of twisting

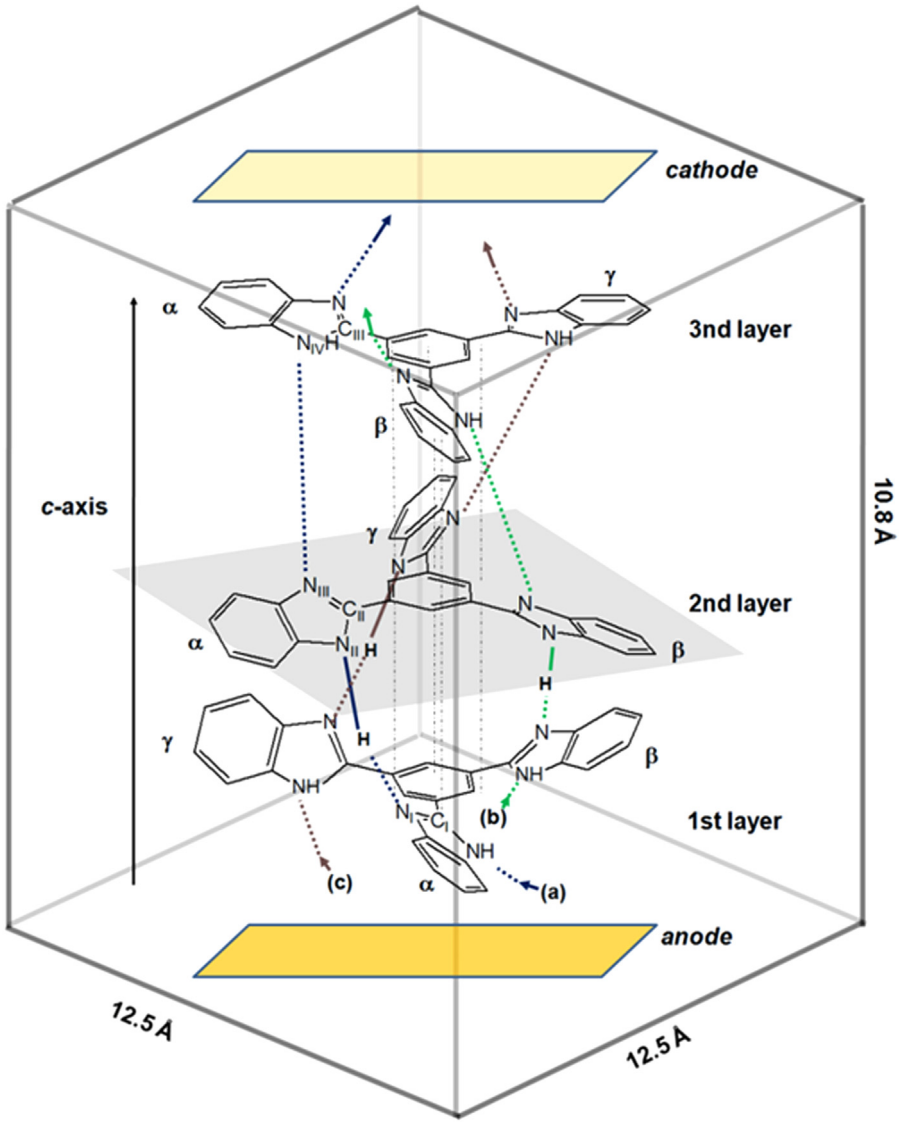

Fig. 4. Schematic representation of proton hopping in periodic type II system: (a), (b) and (c) represent proton hopping at α, β and γ-BENZIM, respectively; the inter-molecular torsion angle of the benzimidazole ring between the I and II layer is Φ_1 (C_I–N_I–N_{II}–C_{II}) and that between the II and III layer is Φ_2 (C_{II}–N_{III}–N_{IV}–C_{III}).

angle and intermolecular distance was analyzed along the reaction coordinate. The energy barrier for proton transfer was found to be 6.45 kJ/mol, as shown in Table 1. The energy of the product decreased after the proton was transferred (− 10.18 kJ/mol).

3.1.2. *Proton transfer under the influence of an electric field*

The effect of an external electric field on the type-I model was studied in detail. The effects of the electric field on the change of R_{N-N} and Φ were measured, as shown in Table 2. The external electric field was found to reduce the distance R_{NI-NII} in the reactant to make the proton transfer more easily. The Φ of the reactant was slightly altered to reduce the distance R_{NI-NII} of the reactant when the external electric field was present. In the product, R_{NI-NII} increased to stabilize the product and retain the proton from I-layer (N_I). To further understand the effect of the external electric field on the intrinsic charge delocalization because of the hydrogen bond, the Hirshfeld charge distribution (Geldof et al., 2011; Van Damme et al., 2009; Marenich et al., 2012; Krishtal et al., 2006) was analyzed. The partial negative charges on N_I (N_i···H) decreased while the partial negative charges on N_{II} (H···N_{II}) increased at the transition state (TS) as higher electric field strengths were applied. The positive partial charge of the proton increased when it moved to N_{II}, resulting in a decrease of partial negative charge on N_I and an increase of partial negative charge on N_{II}. We have performed the calculations to study the effect of the electric field. The calculated energy barriers are 5–6 kJ mol^{-1} following the introduction of an external electric field. Further, not only do we observe a decrease of the energy barriers, we also observe changes to the charge, distance, and torsional angles that

Table 1
Energy, N_I–N_{II} distance (R_{NI-NII}), N_I–H distance (R_{NI-H}), H–N_{II} distance (R_{H-NII}) and inter-molecular torsion angle (Φ) of structures along the estimated reaction path for the type I model.

Structure	Relative energy (kJ/mol)	Distance (Å)			Φ (deg)
		R_{NI-NII}	R_{NI-H}	R_{H-NII}	
Reactant	0.00	2.77	1.09	1.68	−39.87
Transition state	6.48	2.64	1.30	1.35	−40.94
Product	−10.18	2.82	1.75	1.07	−36.09

Table 2
Energy barriers, Hirshfeld charges of N_I, N_{II} at the transition state, change of Φ and N_I–N_{II} distance in the TBIB pair model (type I) under an external electric field.

Electric field (a.u.)	Energy barrier (kJ/mol)	TS atomic charge		Reactant		Transition state		Product	
		N_I	N_{II}	$R_{(NI–NII)}$ (Å)	Φ (deg)	$R_{(NI–NII)}$ (Å)	Φ (deg)	$R_{(NI–NII)}$ (Å)	Φ (deg)
0.0000	6.48	−0.079	−0.096	2.77	−39.87	2.64	−40.94	2.82	−36.09
0.0001	6.30	−0.079	−0.096	2.77	−39.84	2.64	−40.95	2.83	−35.86
0.0010	5.18	−0.072	−0.104	2.76	−42.10	2.65	−40.72	2.85	−32.98
0.0020	5.15	−0.071	−0.105	2.72	−43.14	2.64	−41.05	2.85	−32.65

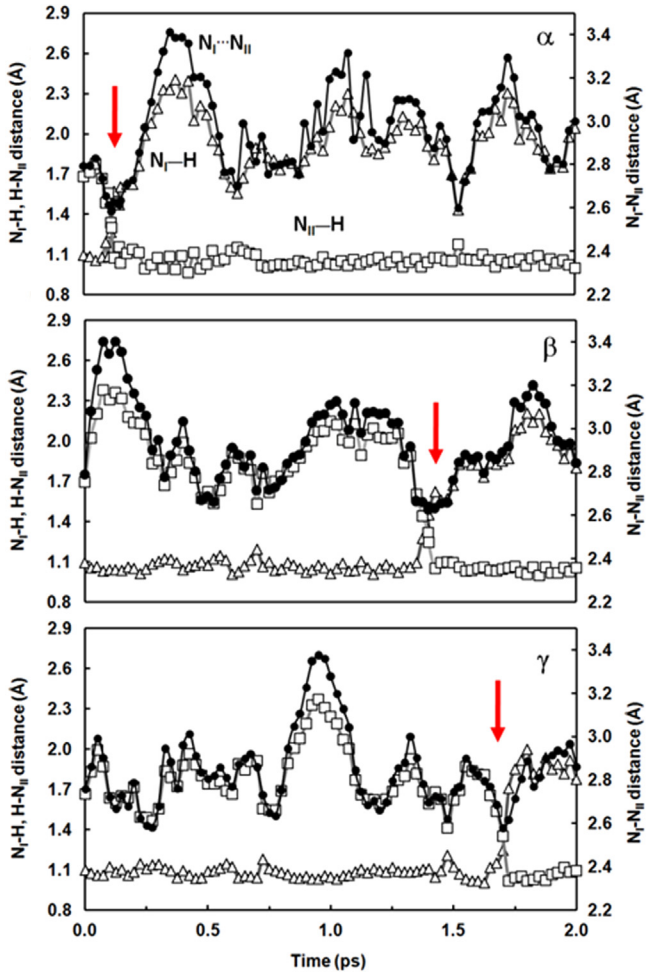

Fig. 5. Change in the N_I–N_{II}, N_I–H and H–N_{II} bond distances for α-BENZIM, β-BENZIM and γ-BENZIM in the TBIB type II model: N_I–H (-Δ-), H–N_{II} (-□-) and N_I–N_{II} (-•-) (For interpretation of the references to color in this figure, the reader is referred to the web version of this article).

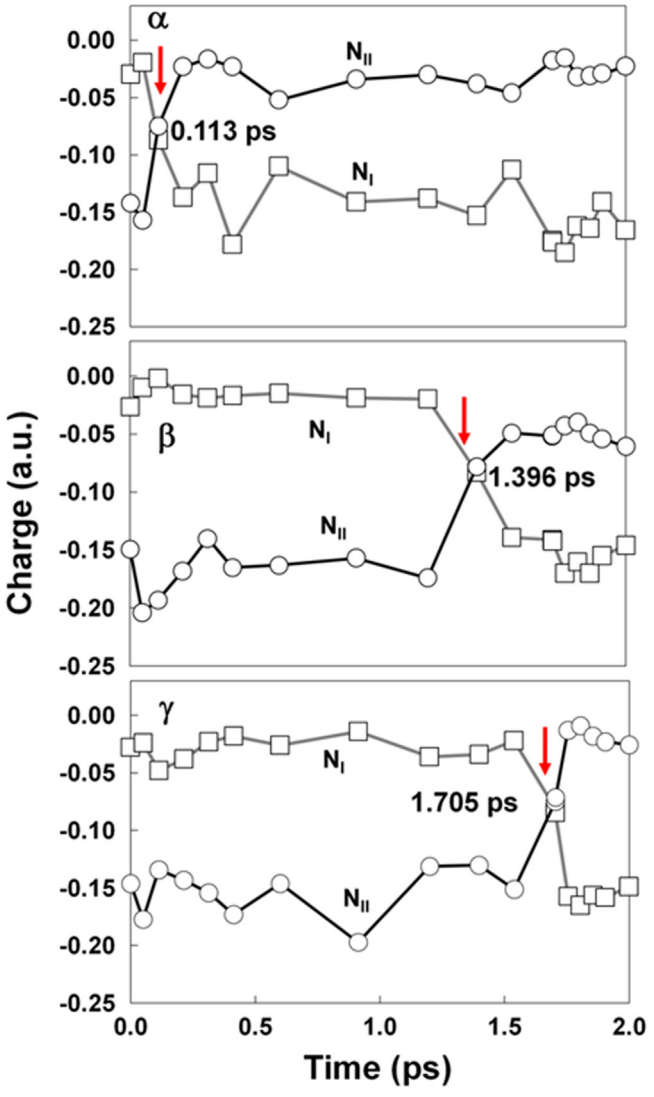

Fig. 6. The crossing of the Hirshfeld charge distribution of N_I and N_{II} at α-BENZIM, β-BENZIM and γ-BENZIM in TBIB type II model: N_I (-□-) and N_{II} (–O-)

assist proton transfer at higher fields. However, more statistics on these results should be obtained to corroborate these findings.

3.2. Proton transfer in the periodic system (type-II model)

3.2.1. Proton transfer path and partial charge distribution

The proton transfer was investigated for the periodic system (type-II Model) shown in Fig. 4 using DFT-MD simulations. Three additional protons were introduced to follow the proton transfers at the three different positions of the three benzimidazole rings: α-BENZIM, β-BENZIM and γ-BENZIM (Fig. 4). The protons were judged as being transferred from one layer to another layer by verifying the exchange of the N_I–H and N_{II}–H distances, as shown in Fig. 5. The calculated trajectories indicate that the N_I–H and N_{II}–H distances exchange at 0.113 ps for α-BENZIM, 1.396 ps for β-BENZIM and 1.705 ps for γ-BENZIM, as indicated by the red arrows. The N_I···N_{II} distance reached the critical value 2.5–2.6 Å at these timings.

The Hirshfeld charge analysis indicates that the charge of N_I and N_{II} exchanges alongside the proton transfer (Fig. 6). The coherent switching of these parameters was found to occur in association with a fluctuation of the inter-molecular torsional angle, as shown in Fig. 7. These calculations indicate that proton transfer may proceed via a stepwise mechanism and not via the simultaneous hopping process between these three rings.

The distribution of the torsional angle Φ_1 of the benzimidazole ring with and without the transferred protons is shown in Fig. 8. In the case of the α-ring, the torsional angle distributes around −33° when the α-ring

possesses the proton, which shifts to -13° in the absence of the proton. The γ-ring shows a similar shift from -38° to -2°. That is to say, as illustrated in Fig. 8 (on the right), the proton transfer process occurs through the hydrogen bond network and the proton moves from the ring in the lowest layer to the second layer by inducing a slight change of the inter-molecular torsional angle. This torsional motion of the rings is smaller than that observed for imidazole (Kreuer et al., 1998; Münch et al., 2001; Nimmanpipug et al., 2013), indicating that a rather rigid structure of TBIB molecules stabilizes the helical hydrogen-bond networks and restrains the twisting of the benzimidazole ring during proton transfer. A reorientation of the ring is limited but the proton diffusion coefficient is higher than those reported previously for water and imidazole (Kreuer et al., 1998; Münch et al., 2001; Nimmanpipug et al., 2013).

As discussed in these two sections, proton hopping was found to occur when the inter-molecular distance ($N_I \cdots N_{II}$) reached a critical distance (*i.e.*, ~2.5–2.6 Å) and the length of the N_I–H and H–N_{II} bonds were exchanged. Additionally, the torsional motion of the imidazole ring is found to be important in causing these geometrical changes.

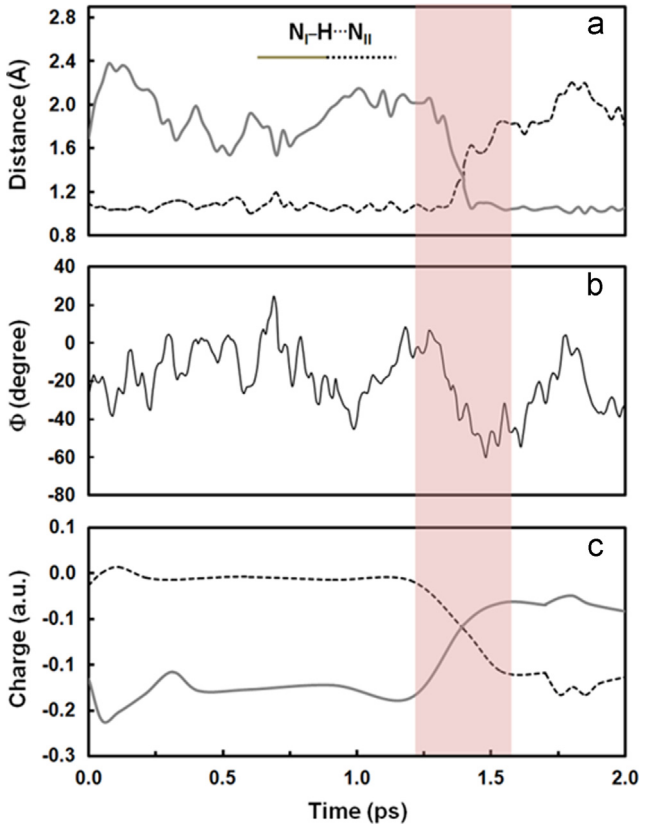

Fig. 7. Switching of (a) distance (—N_I–H and — H–N_{II}), (b) inter-molecular torsion angle (Φ) and (c) Hirshfeld charge distribution (—N_I and — N_{II}) of TBIB as a function of simulation time for β-BENZIM in the type-II model.

3.2.2. Proton transfer under an external electric field

3.2.2.1. Distance change in each possible position. The change of the N_I–N_{II}, N_I–H and H–N_{II} bond distances was analyzed from the results of the molecular dynamics simulations under the influence of an external electric field. Fig. 9 shows the effect of the electric field on the timings of the proton hopping. The proton hopping occurs more quickly when the applied electric field strength became higher, although the effect varies with the specific ring.

3.2.2.2. Dynamic behavior of a proton under the influence of an external electric field. To explain the behavior of a proton under the influence of an external electric field, the diffusion coefficient of the proton was determined. The proton diffusion coefficient in the hopping process was calculated from the slope of MSD plotted against time (Kreuer et al., 1998; Kubo, 1957) and is listed in Table 3. In TBIB, charge mobility is 820, 1447 and 1196 $Å^2\ ps^{-1}$ $a.u.^{-1}$ for external electric fields of 0.0025, 0.005 and 0.005 a.u., respectively. The results indicate that the electric field can enhance proton mobility along the hydrogen-bonding path to give a higher diffusion coefficient to the hopping proton. Relative to the data for water and imidazole, a high inherent capacity of TBIB as an alternative electrolyte is suggested by this calculation.

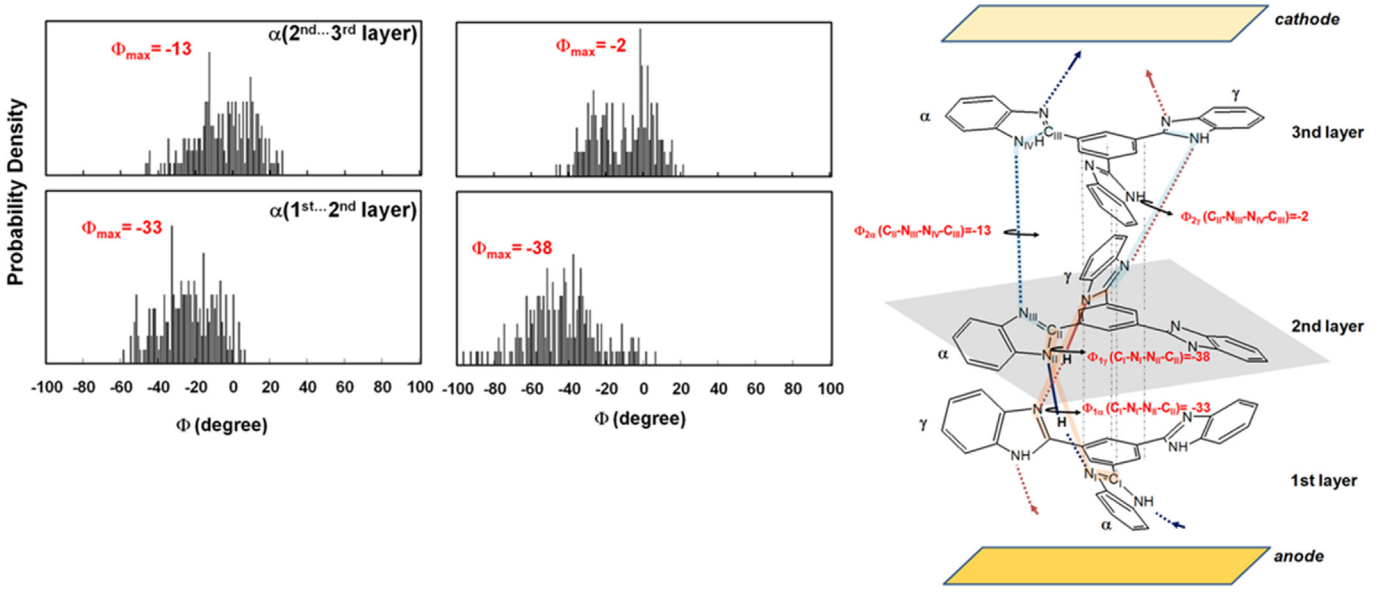

Fig. 8. Distribution of Φ for α-BENZIM and γ-BENZIM (C_I–N_I–N_{II}–C_{II}); the ring engaging proton hopping, α-BENZIM and γ-BENZIM, and the normal ring (no proton transfer observed), α-BENZIM and γ-BENZIM.

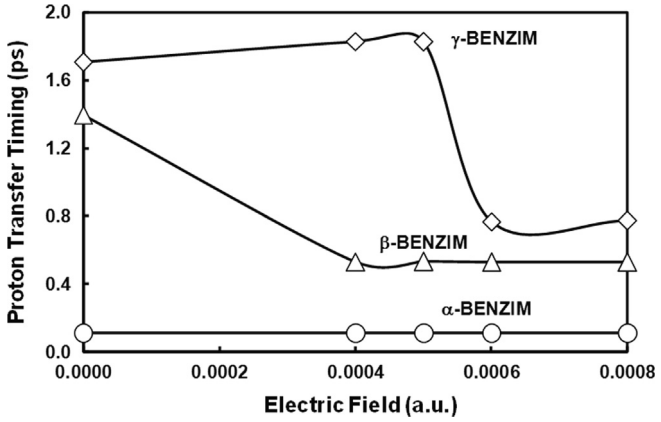

Fig. 9. Proton transfer timings of three projections (α:–O-, β:-Δ- and γ:-◇–BENZIM) following the introduction of an external electric field.

Table 3
Diffusion coefficients of a proton in the TBIB model (type II) under the influence of an external electric field.

Electric field (a.u.)	Diffusion coefficient (Å^2/ps)		
	Water (Nimmanpipug et al., 2013)	Imidazole (Nimmanpipug et al., 2013)	TBIB
0.0000	0.176	0.106	0.098
0.0025	2.452	N/A	2.051
0.0050	3.513	2.123	7.236
0.0060	N/A	N/A	7.175

4. Conclusions

Density functional molecular dynamics simulations were utilized to investigate proton transfer along the unique three-dimensional hydrogen bond network in TBIB. Two different models were extracted from the X-ray crystal structure so that the essential key points could be discerned easily. For the type I model, transition state searches based on crystallographic data for TBIB revealed a relatively low energy barrier of 6.45 kJ/mol for the proton hopping processes. The application of an external electric field accelerates the proton transfer drastically by lowering the energy barrier and stabilizing the proton acceptor. Partial charge analysis suggests that the external electric field is a crucial driving force in promoting proton mobility along the hydrogen bond direction. In the three-molecular system with a periodic columnar structure (type II) the DFT-MD simulations indicated that the protons transfer at various timings between the three rings: 0.113, 1.396, and 1.705 ps for α-, β-, and γ-BENZIM, respectively. The structural arrangement during the molecular dynamics simulations suggests a consecutive proton transfer pathway occurring from α-, β-, and then to γ-BENZIM. The crystal structure of TBIB is stabilized by a three-stranded helical hydrogen bonding structure. As a result, the reorientation amplitude of the rings is limited, but its proton diffusion coefficient is higher than the analogous coefficient for water and imidazole, indicating that the proton transfers with high efficiency along the highly organized hydrogen-bonding network of TBIB. These results correlate well with the experimental NMR spectroscopic results that suggest that the hydrogen bond network induces a relatively tight packing structure in TBIB (Pangon et al., 2011). Thus, the cause of the exceptionally high measured proton conductivity of TBIB can be understood quite reasonably from the present DFT-MD calculations.

5. Funding sources

The work was partially supported by the Mid-Career Researcher Fund of Chiang Mai University, Thailand, the Thailand Graduate Institute of Science and Technology (TGIST), and the Centre for Innovation in Chemistry (PERCH-CIC), Thailand.

Acknowledgments

The work was partially supported by the Mid-Career Researcher Fund of Chiang Mai University, Thailand, the Thailand Graduate Institute of Science and Technology (TGIST), and the Centre for Innovation in Chemistry (PERCH-CIC), Thailand.

References

Agmon, N., 1995. Chem. Phys. Lett. 244, 456.
Chen, H., Yan, T., Voth, G.A., 2009. J. Phys. Chem. A 113, 4507.
Choi, P., Jalani, N.H., Datta, R., 2005. J. Electrochem. Soc. 152, E123.
Devanathan, R., 2008. Energy Environ. Sci. 1, 101.
Geldof, D., Krishtal, A., Blockhuys, F., Van Alsenoy, C., 2011. J. Chem. Theory Comput. 7, 1328.
Gosalawit, R., Chirachanchai, S., Manuspiya, H., Traversa, E., 2006. Catal. Today 118, 259.
Hermansson, K., Ojamäe, L., 1995. Solid State Ionics 77, 34.
Isaev, A.N., 2012. Russ. J. Phys. Chem. 86, 69.
Ishikita, H., Saito, K., 2014. J. R. Soc. Interface 11, 20130518.
Jeong, S.U., Cho, E.A., Kim, H.-J., Lim, T.-H., Oh, I.-H., Kim, S.H., 2006. J. Power Sources 158, 348.
Kawada, A., McGhie, A.R., Labes, M.M., 1970. J. Chem. Phys. 52, 3121.
Kreuer, K.D., Fuchs, A., Ise, M., Spaeth, M., Maier, J., 1998. Electrochim. Acta 43, 1281.
Krishtal, A., Senet, P., Yang, M., Van Alsenoy, C., 2006. J. Chem. Phys. 125, 34312.
Kubo, R., 1957. J. Phys. Soc. Jpn. 12, 570.
Li, A., Cao, Z., Li, Y., Yan, T., Shen, P., 2012. J. Phys. Chem. B 116, 12793.
Ludueña, G.A., Kühne, T.D., Sebastiani, D., 2011. Chem. Mater. 23, 1424.
Marenich, A.V., Jerome, S.V., Cramer, C.J., Truhlar, D.G., 2012. J. Chem. Theory Comput. 8, 527.
Münch, W., Kreuer, K.D., Silvestri, W., Maier, J., Seifert, G., 2001. Solid State Ionics 145, 437.
Nimmanpipug, P., Yana, J., Lee, V.S., Vannarat, S., Chirachanchai, S., Tashiro, K., 2013. J. Power Sources 229, 141.
Ohwaki, T., Yamashita, K., 2001. J. Electroanal. Chem. 504, 71.
Pangon, A., Totsatitpaisan, P., Eiamlamai, P., Hasegawa, K., Yamasaki, M., Tashiro, K., Chirachanchai, S., 2011. J. Power Sources 196, 6144.
Peterson, V.K., Corr, C.S., Boswell, R.W., Izaola, Z., Kearley, G.J., 2013. J. Phys. Chem. C 117, 4351.
Schuster, M., Meyer, W.H., Wegner, G., Herz, H.G., Ise, M., Kreuer, K.D., Maier, J., 2001. Solid State Ionics 145, 85.
Smitha, B., Sridhar, S., Khan, A.A., 2005. J. Membr. Sci. 259, 10.
Studio, M. Accelrys Software Inc. 2011.
Tashiro, K., Pangon, A., Hasegawa, H., Yamazaki, M., Totsatipaisan, P., Chirachanchai, S., 2009. Polym. Prepr. Jpn. 58, 5702.
Tölle, P., Cavalcanti, W.L., Hoffmann, M., Köhler, C., Frauenheim, T., 2008. Fuel Cells 8, 236.
Van Damme, S., Bultinck, P., Fias, S., 2009. J. Chem. Theory Comput. 5, 334.
Yamada, M., Honma, I., 2005. Polymer 46, 2986.
Yan, L., Zhu, S., Ji, X., Lu, W., 2007. J. Phys. Chem. B 111, 6357.